Thomson Scattering from Inertial-Confinement-Fusion Hohlraum Plasmas

S. H. Glenzer,[1] C. A. Back,[1] L. J. Suter,[1] M. A. Blain,[2] O. L. Landen,[1] J. D. Lindl,[1] B. J. MacGowan,[1] G. F. Stone,[1] R. E. Turner,[1] and B. H. Wilde[3]

[1]*L-399, Lawrence Livermore National Laboratory, University of California, P.O. Box 808, Livermore, California 94551*

[2]*Centre D'Etudes de Limeil-Valenton, Villeneuve-Saint-Georges, France*

[3]*Los Alamos National Laboratory, Los Alamos, New Mexico 87545*

(Received 17 March 1997)

We present the first Thomson scattering measurements of local plasma conditions in ignition-relevant, gas-filled, inertial-confinement-fusion hohlraums. The experimental data provide a benchmark for two-dimensional hydrodynamic simulations using LASNEX, which is presently in use to predict the performance of future megajoule laser-driven hohlraums of the National Ignition Facility. The data are consistent with modeling using significantly inhibited heat transport at the peak of the drive. Further, we find that stagnating plasma regions on the hohlraum axis are well described by the calculations. [S0031-9007(97)03841-6]

PACS numbers: 52.58.Ns, 52.40.Nk, 52.65.Kj, 52.70.Kz

A key issue for the ignition of indirectly driven inertial confinement fusion (ICF) capsules is the controlled deposition of energy into a radiation cavity (hohlraum) and a symmetric high-convergence implosion of the capsule [1]. Using large glass laser drivers, as planned for the National Ignition Facility (NIF), present hydrodynamic simulations show that more than 1 MJ of laser energy has to be delivered with a shaped laser pulse into a cylindrical centimeter-size high-Z hohlraum [2]. A high-Z plasma is created at the hohlraum wall where the laser energy converts into soft x rays which heat and implode a deuterium-tritium filled spherical capsule. Present ignition designs [2,3] use hohlraums filled with a low-Z gas [4,5] to reduce inward motion of the high-Z wall plasma and to obtain high soft x-ray radiation symmetry which is necessary to achieve high capsule convergence.

In this Letter, we present the first Thomson scattering measurements [6,7] within closed geometry, hohlraum targets. These experiments provide the first direct and accurate measurement of the electron temperature T_e, ion temperature T_i, and plasma flow $\mathbf{v}$ of the low-Z plasma in ignition-relevant, gas-filled, hohlraums [8–10], thus benchmarking hydrodynamic simulations. The experimental quantities are important parameters to understand the energetics of hohlraums and physical processes such as beam pointing [11] and stagnation processes which influence the capsule implosion in indirect drive experiments.

Radiation hydrodynamic simulations of both NIF and Nova hohlraums are carried out with the LASNEX [12] computer code which uses a flux-limited diffusion model for heat transport. In this approximation heat flow per unit area in regions of large classical heat flow ($-\kappa\nabla T_e$) has an upper bound of $f(n_e T_e v_e)$, where $n_e T_e v_e$ is the so-called free streaming value of heat transport and f is the flux limit. Flux limiters of $0.01 < f < 0.1$ have been found necessary to model laser-heated disk experiments [13] where steep temperature gradients near the disk surface cause classical heat flow to become unphysically large. In laser-heated hohlraums, however, the confined geometry results in very different temperature and density profiles so that the heat flow is flux limited over the volume of the hot plasma. For that reason, equivalent results can be obtained by merely reducing the classical transport coefficient.

The present hohlraum experiments show a steep rise of the electron temperature to 5 keV at the peak of the drive that is consistent with calculations only by strongly inhibiting the heat transport. A temperature of $T_e =$ 5 keV can be approximated with a flux limiter of $f =$ 0.01 or an equivalent reduction of the classical transport by a factor of 10. While this finding is not presently understood, it does indicate that it is necessary to include heat transport limiting effects into the modeling, e.g., magnetic fields [14,15] or nonlocal transport [16].

The experiments were performed using cylindrical gold hohlraums heated with 21–25 kJ of 351 nm (3ω) laser light at the Nova Laser Facility [17]. The hohlraums were 2750 μm long with a radius of 800 μm (scale 1) which is a standard target for capsule implosions. We used 1 atm of methane (CH_4) as gas fill giving an initial electron density of $n_e = 2.7 \times 10^{20}$ cm^{-3} when fully ionized. The hohlraums were heated with eight or nine unsmoothed heater beams of the Nova laser that are arranged in cones on either side of the hohlraum so that each beam forms an angle of 50° to the hohlraum axis. The heater beams penetrate the hohlraum at both ends through laser entrance holes of 600 μm radius (Fig. 1) which are covered with 0.35 μm thick polyimide membranes. The beams cross at the center of the holes and are diverging so that they produce an elliptical spot on the hohlraum wall of about 700 μm $\times$ 500 μm size. We applied shaped laser pulses of 2.2 ns duration which rise from 0.6–1.8 TW per beam (cf. Fig. 1).

Thomson scattering was performed with one of the Nova laser beams which was $\lambda_i = 526.6$ nm (2ω) and was a 4 ns square pulse of frequency converted to

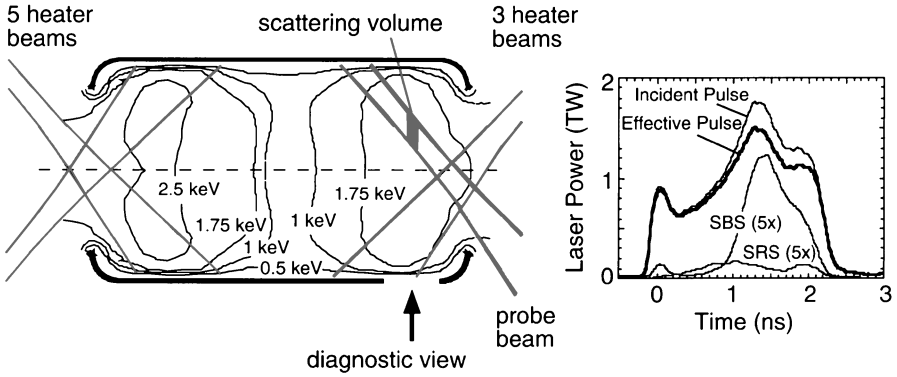

FIG. 1. Schematic of the experimental setup. An electron temperature contour calculated by LASNEX for a gas-filled hohlraum without a capsule is included for $t = t_0 + 0.8$ ns. The location of the scattering volume indicated by the shaded area is in a rather homogeneous part of the CH plasma. The scattering angle between the probe beam and the direction of observation is 104°. Also shown is the laser power of a single beam together with measured SRS and SBS losses. The total energy loss is 14%.

constant power (0.1–0.4 TW). The scattering volume is 400 μm inside of the hohlraum (Fig. 1). The Thomson scattered light is observed through a diagnostic window (700 μm $\times$ 400 μm) which is cut into the hohlraum wall and also covered with polyimide. The scattering volume is imaged at $\times 1.5$ magnification onto the entrance slit of a 1-m spectrometer which is equipped with a 1200 lines/mm grating. Spectra were recorded in second spectral order with a wavelength resolution of 0.1 nm and a temporal resolution of 30 ps using an optical streak camera. High spatial discrimination of 133 μm in the vertical direction of the hohlraum and 66 μm in the axial direction was obtained by choosing the entrance slit width of the spectrometer to be 200 μm and by employing a streak camera slit height of 100 μm.

We have performed two-dimensional hydrodynamic simulations [10,12] of this experiment. Five heater beams were modeled on one side of the hohlraum and three or four heater beams were included on the other side where Thomson scattering was performed. The probe laser has a relatively low power and we find experimentally no influence of the probe laser on the plasma conditions when varying its intensity by almost 1 order of magnitude. For that reason it was neglected in the simulations. The heater beam power used in the modeling was taken from the measured incident beam power corrected for measured stimulated Brillouin (SBS) and Raman (SRS) backscattering and near backscattering losses using techniques described in Refs. [18,19] (Fig. 1). For typical electron temperatures and densities of hohlraums, collective Thomson scattering spectra are expected; scattering parameters are $\alpha = 1/k\lambda_D \sim 3$, where $\mathbf{k}$ is the scattering vector and λ_D the Debye length of the plasma [6].

Figure 2(a) shows a temporally resolved collective Thomson scattering spectrum from a hohlraum heated with eight heater beams of 21 kJ energy. For $t_0 < t < t_0 + 0.65$ ns, where t_0 denotes the beginning of the heating, no Thomson scattering signal can be observed. Estimates show that during this time the polyimide foil which covers the diagnostic window produces an overdense plasma for 2ω light. During that time a faint line due to stray light or unconverted 2ω light from the heater beams can be identified in Fig. 2. It provides a convenient timing and wavelength fiducial. For $t_0 + 0.65$ ns $< t < t_0 + 1.1$ ns two broad symmetric ion acoustic features are observed from light scattering off the CH_4 plasma. For $t_0 + 1.1$ ns $< t < t_0 + 1.6$ ns, when the heater beam power rises significantly (Fig. 1), the separation of the ion acoustic features increases indicating a rising electron temperature and, in addition, the width of the ion acoustic features narrows showing an even faster increase of the ion temperature of the plasma. Furthermore, the spectrum shows an asymmetry probably related to electron heat flux towards the hohlraum wall which would result in different electron Landau damping of the co- and counterpropagating ion acoustic waves [20]. For $t > t_0 + 1.6$ ns, a cutoff of the Thomson scattering signal occurs because the electron density of the CH plasma rises steadily during the heating of the hohlraum due to compression by the inward-moving wall plasma.

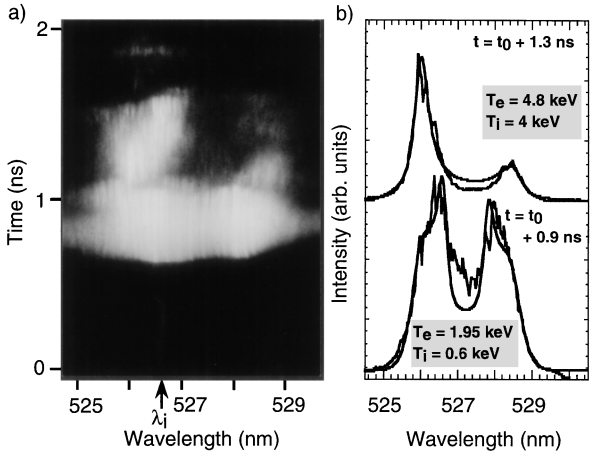

FIG. 2. Time-resolved Thomson scattering spectrum for eight heater beams (a). The spectra are fitted with the form factor of Evans [21] giving electron and ion temperatures (b).

Figure 2(b) shows the spectra at $t = t_0 + 0.9$ ns and $t = t_0 + 1.3$ ns averaged over 80 ps together with a fit using the form factor of Evans [21]. For the data analysis it is assumed that light scattering occurs on a fully ionized CH plasma. Our hydrodynamic simulations as well as temporally resolved two-dimensional x-ray images observing the Au-plasma emission show that Au ions were not present in the scattering volume for $t < t_0 + 1.7$ ns. The Thomson scattering spectra consist of four features: Two co- and counterpropagating ion acoustic waves belonging to C (slow wave) and to H (fast wave) [22,23]. The fit to the data yields the separation and the relative damping of both waves measuring accurately the electron and ion temperature of the plasma [22].

Figure 3 shows the temporal evolution of the electron temperature from Thomson scattering along with the results of the simulations. Data are shown for eight heater beams [Fig. 3(a)] and for nine heater beams [Fig. 3(b)]. The experimental electron temperatures clearly scale with the number of heater beams. We observe peak values of 4.5 and 5.2 keV, respectively. The reproducibility of the hohlraum plasma conditions is about 20%. Varying the probe laser focus in the range of 150 to 500 μm diameter at the scattering volume did not affect the experimental temperatures. This result is consistent with LASNEX calculations which show a rather homogeneous electron temperature about 400 μm inside of the hohlraum (Fig. 1).

For the analysis we have calculated the scattering parameter α using electron densities from LASNEX. Although for the present experiment we have $\alpha \sim 3$ so that the spectra are not density sensitive, the **k** vector was slightly corrected from its vacuum value [24] since electron densities in the scattering volume approach $0.25 n_{cr}$, where n_{cr} is the critical density for the 2ω probe. Ignoring this effect would result in electron temperatures reduced by 10%–20%. The density correction introduces an additional uncertainty to the experiment resulting in a total error bar of 15% for T_e and 20% for T_i.

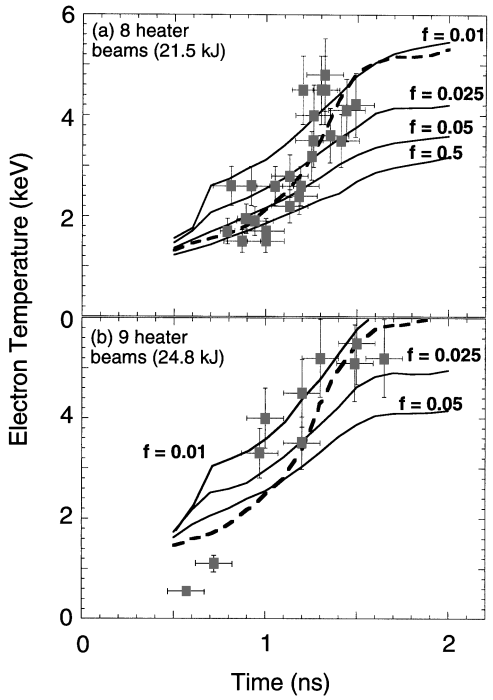

FIG. 3. Hohlraum electron temperatures as a function of time for eight (a) and nine (b) heater beams together with hydrodynamic simulations with various flux limiters.

In Fig. 3 calculations are shown for various (constant) free streaming electron heat transport flux limiters in the range of $f = 0.5$–$f = 0.01$. For example, using $f = 0.025$ agrees with the experimental electron temperatures to within 35%. However, the best description of the experimental data is obtained when assuming a time-varying flux limiter of $f = 0.1$ at early times decreasing to $f = 0.01$ at the peak of the drive (dashed curve in Fig. 3). Alternatively, we can model the experiment with classical transport reduced by a factor of 5–10. For gas-filled hohlraum plasmas, electron heat transport inhibition due to magnetic fields by a factor of about 20 was predicted in Ref. [14]. Also, nonlocal heat transport [16] could be important for the present observations. Experiments and calculational efforts are presently ongoing to better understand and quantify these effects.

The Thomson scattering data also give information about macroscopic plasma flow in hohlraums which is an important parameter affecting beam pointing [11]. In Fig. 2 we observe a redshift of the spectra due to plasma motion away from the heater beam spots on the hohlraum wall. The speed is subsonic ($v = 4.3 \times 10^7$ cm/s) and underestimated by the two-dimensional simulations by a factor of 2–3. This Doppler shift (as well as the heat-flux driven asymmetry) is a three-dimensional effect and occurs when employing only eight heater beams. When applying nine heater beams, the redshift of the spectra decreases to about 20% of the sound speed ($v = 1.4 \times 10^7$ cm/s) and the spectra become symmetric because of the improved symmetry of the hohlraum heating. In this case, agreement of the flow velocity with the hydrodynamic simulations is obtained within 30%. Unfortunately, the Thomson scattering spectra with nine heater beams show increased stray light levels since the additional heater beam illuminates part of the diagnostic window.

Figure 4 shows the ion temperature as a function of time for eight [Fig. 4(a)] or nine [Fig. 4(b)] heater beams. Ion temperatures are less sensitive to the flux limiter. The experimental ion temperatures show a steep rise to a peak value of 4 keV. From the hydrodynamic simulations we deduce that this behavior is due to stagnation of the compressed low-Z plasma on the axis of the hohlraum. Electron-ion temperature equilibration times are too large (>1 ns) to explain the experimental data. In Fig. 4(a) the simulated ion temperature rise is delayed compared to the experimental data by ~0.4 ns while in case of nine heater beams [Fig. 4(b)] a delay of ~0.2 ns occurs. These observations can be explained by the fact that the hydrodynamic simulations are two dimensional and

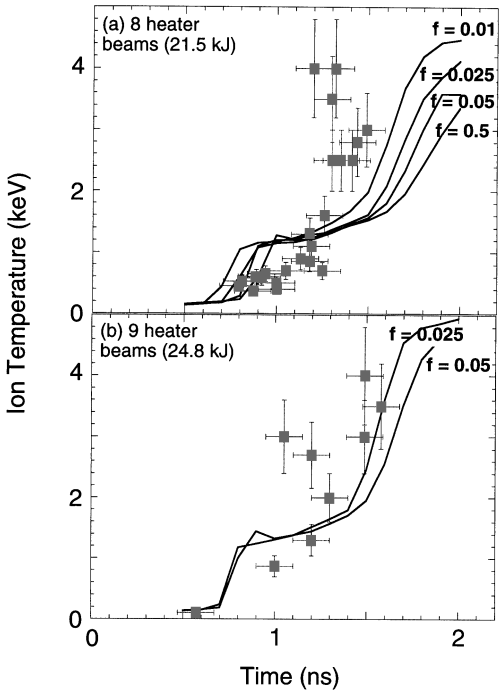

FIG. 4. Same as Fig. 3 for the ion temperature ($T_C = T_H$).

assume a cylindrical symmetric heating. However, in the case of eight heater beams the heating is fairly asymmetric so that the plasma stagnates slightly off axis closer to the Thomson scattering volume giving rise to an earlier ion temperature increase than seen in the simulations. In case of nine heater beams the symmetry of the heating is improved and stagnation occurs closer to the hohlraum axis so that the beginning of the ion temperature rise is better described by the LASNEX simulations.

Besides being important for affecting the level of parametric instabilities in hohraums, the high temperature plasmas in hohlraums generate significant pressure which can affect the capsule dynamics under some circumstances. For example, early NIF hohlraums used plastic liners [1] instead of a gas fill. They blew inward at high velocity and generated an early time axial stagnation pressure which affected the subsequent capsule implosion symmetry. However, in the gas-filled hohlraums, the high gas pressures occur late, after the capsule has generated a large surrounding region of ablated material. In these hohlraums, there is virtually no affect of the gas-region pressure on the capsule implosion. Because the capsule is moving inward and the radiation ablated capsule blowoff is moving outward at speeds comparable to the sound speed in the gas fill, the capsule is essentially isolated from the pressure generated in the gas. This is true for both the Nova experiments and for the NIF target designs. In NIF calculations, the capsules have essentially the same symmetry and implosion velocity in integrated calculations which explicitly account for the low-Z gas pressure [2,3,10] and in separate calculations which only drive the capsule with the hohlraum x-ray flux. When a reduced flux limiter of $f = 0.01$ is used in NIF calculations, the optimal beam power is slightly modified because of the changed plasma conditions, but otherwise the calculations are unaffected.

In conclusion, we have measured plasma parameters of indirectly driven ignition-relevant ICF hohlraums with Thomson scattering. The detailed comparison with two-dimensional hydrodynamic LASNEX modeling shows that ion temperatures and plasma flow, i.e., quantities which are not sensitive to the choice of the heat transport flux limiter, agree quite well with the simulations. The experimental electron temperatures are best approximated with a time-varying flux limiter showing large electron heat transport inhibition at the peak of the drive. This observation is presently not understood and will hopefully motivate the inclusion of heat transport limiting effects into the hydrodynamic modeling.

We acknowledge helpful discussions with E. M. Campbell, R. L. Berger, M. D. Rosen, B. B. Afeyan, K. G. Estabrook, R. K. Kirkwood, and J. D. Moody. This work was performed under the auspices of the U.S. Department of Energy under Contract No. W-7405-ENG-48.

[1] J. D. Lindl, Phys. Plasmas **2**, 3933 (1995).
[2] S. W. Haan *et al.*, Phys. Plasmas **2**, 2480 (1995).
[3] W. J. Krauser, Phys. Plasmas **3**, 2084 (1996).
[4] L. V. Powers *et al.*, Phys. Rev. Lett. **74**, 2957 (1995).
[5] C. A. Back *et al.*, Phys. Rev. Lett. **77**, 4350 (1996).
[6] H.-J. Kunze, in *Plasma Diagnostics*, edited by W. Lochte-Holtgreven (North-Holland, Amsterdam, 1968), p. 550.
[7] A. W. DeSilva and G. C. Goldenbaum, in *Methods of Experimental Physics*, edited by H. R. Griem and R. Lovberg (Academic, New York, 1967), Sect. V9A.
[8] B. A. Hammel *et al.*, Phys. Rev. Lett. **70**, 1263 (1993).
[9] R. L. Kauffman *et al.*, Phys. Rev. Lett. **73**, 2320 (1994).
[10] L. J. Suter *et al.*, Phys. Rev. Lett. **73**, 2328 (1994).
[11] H. S. Rose, Phys. Plasmas **3**, 1709 (1996); J. D. Moody *et al.*, Phys. Rev. Lett. **77**, 1294 (1996); D. S. Hinkel *et al.*, Phys. Rev. Lett. **77**, 1298 (1996).
[12] G. B. Zimmerman and W. L. Kruer, Comments Plasma Phys. Control. Fusion **2**, 85 (1975).
[13] D. S. Montgomery *et al.*, Phys. Rev. Lett. **73**, 2055 (1994); S. H. Batha *et al.*, Phys. Plasmas **2**, 3792 (1995); S. H. Glenzer *et al.*, Rev. Sci. Instrum. **68**, 668 (1997).
[14] S. E. Bodner, Comments Plasma Phys. Control. Fusion **16**, 351 (1995).
[15] J. A. Stamper and B. H. Ripin, Phys. Rev. Lett. **34**, 138 (1975); J. Hammer and L. Powers (private communication); M. G. Haines, Phys. Rev. Lett. **78**, 254 (1997).
[16] J. R. Albritton *et al.*, Phys. Rev. Lett. **57**, 1887 (1986); J. F. Luciani, Phys. Fluids **28**, 835 (1985); A. R. Bell *et al.*, Phys. Rev. Lett. **46**, 243 (1981).
[17] E. M. Campbell *et al.*, Rev. Sci. Instrum. **57**, 2101 (1986).
[18] B. J. MacGowan *et al.*, Phys. Plasmas **3**, 2029 (1996).
[19] R. K. Kirkwood *et al.*, Phys. Plasmas **4**, 1800 (1997).
[20] V. T. Tikhonchuk *et al.*, Phys. Plasmas **2**, 4169 (1995).
[21] D. E. Evans, Plasma Phys. **12**, 573 (1970).
[22] S. H. Glenzer *et al.*, Phys. Rev. Lett. **77**, 1496 (1996).
[23] E. A. Williams *et al.*, Phys. Plasmas **2**, 129 (1995).
[24] B. La Fontaine *et al.*, Phys. Plasmas **1**, 2329 (1994).